



Synthesis and cytotoxic analysis of thiolated xylose derivatives decorated on gold nanoparticles

Angus Shiue^{a,1}, Jenn-Han Chen^{b,1}, Chia-Ying Chang^a, Shu-Mei Chang^{a,c,d,*}, Kuo-Yuan Hwa^{a,c,e,*}, Kai-Yen Chin^a, Graham Leggett^f

^a Graduate Institute of Organic and Polymeric Materials, National Taipei University of Technology, Taipei, Taiwan

^b Graduate Institute of Clinical Medicine, Taipei Medical University, Taipei, Taiwan

^c Department of Molecular Science and Engineering, National Taipei University of Technology, Taipei, Taiwan

^d Research and Development Center for Smart Textile Technology, National Taipei University of Technology, Taipei, Taiwan

^e Center for Biomedical Industry, National Taipei University of Technology, Taipei, Taiwan

^f LI-COR Biosciences, Cambridge, England



ARTICLE INFO

Article history:

Received 6 August 2020

Received in revised form 20 October 2020

Accepted 29 October 2020

Keywords:

Gold nanoparticles

Surface

Plasmon resonance

Xylose

ABSTRACT

The rapid development of metal nanoparticles capped by an organic monolayer offers the possibility to create a whole new variety of products with novel characteristic, functions and applications. Among these, nanoparticles covered with carbohydrates (glyconanoparticles) constitute a good bio-mimetic model of carbohydrate presentation at the cell surface and are currently centered on many glycobiological and biomedical applications. In this study, a series of novel D-xylose gold nanoparticles (AuNPs) with linkages of alkyl or polyethylene glycol have been synthesized via D-xylosethiols, forming self-assembled monolayers on gold nanoparticles. The nano-gold solution, two carbohydrate derivatives and modified nano-gold solution were tested for cytotoxicity to check the biocompatibility. The MTT assay on NIH 3T3 cell lines confirmed that all the test materials showed no toxicity with the more than 90 % of cell viability in both low concentration (1 μ M) and high concentration (100 μ M), compared with the control.

© 2020 The Authors. Published by Elsevier B.V. This is an open access article under the CC BY-NC-ND license (<http://creativecommons.org/licenses/by-nc-nd/4.0/>).

1. Introduction

The study of nanomaterials is focused at the 1–100 nm scale, involving material manufacturing technology and the properties of new materials. Today, the nanomaterial technology field plays a very important role. While the term nanomaterials came into common usage in the 1980s, research into the development of materials at the 1–100 nm scale had been underway considerably earlier. Metal-based synthetic nanomaterials are nanosized metals such as copper (Cu), iron (Fe), palladium (Pt), gold (Au), aluminium (Al), zinc (Zn) and silver (Ag). Among the large number of metal-based synthetic nanomaterials, gold is one of the primary supports for the production of carbohydrate nanoparticles [1,2]. Gold is an extremely inert and biocompatible material. At the nanoscale, gold nanoparticles (AuNPs) have unique optical properties which are useful in many diagnostic and affinity studies or protocols. In

addition, gold can be easily and covalently decorated on the surface by utilizing the strong soft–soft interaction between Au atoms and sulfur [3]. To date, various synthetic techniques to produce AuNPs, including chemical, thermal, electrochemical and sonochemical pathways, have been introduced [4–7]. In principle, there are two approaches for the synthesis of AuNPs: the “bottom-up” approach and the “top-down” approach [8]. The bottom-up approach includes nanosphere lithography, templating, chemical, photochemical, electrochemical, sonochemical, and thermal reduction techniques [9–13]. However, just a few methods produce particles of uniform size. The most common methods include reducing the acidification of gold salts to produce gold particles of 12–20 nm in a relatively narrow size distribution (standard deviation, –10 to 16 %) [14,15].

Brust et al. [16] applies borohydride reduction of gold salt in the presence of an alkanethiol capping agent to produce 1 – 3 nm particles. Seed growth techniques have been shown to be the exception when it comes to controlling the size of nanoparticles [17,18]. In this technique, the small metal nanoparticles are first prepared and used as seeds (nucleated bits), mixed with a growth solution to synthesize larger particles [19]. Prefabricated seeds and growth solutions inhibit secondary or further nucleation,

* Corresponding authors at: 1, Sec. 3, Chung Hsiao E Road, Taipei, 10608, Taiwan.
E-mail addresses: f10914@mail.ntut.edu.tw (S.-M. Chang),
kyhwa@mail.ntut.edu.tw (K.-Y. Hwa).

¹ Denotes equal contribution

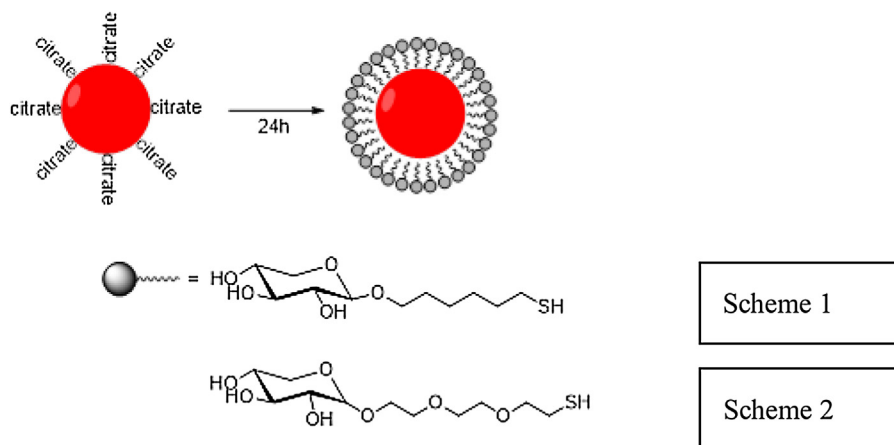
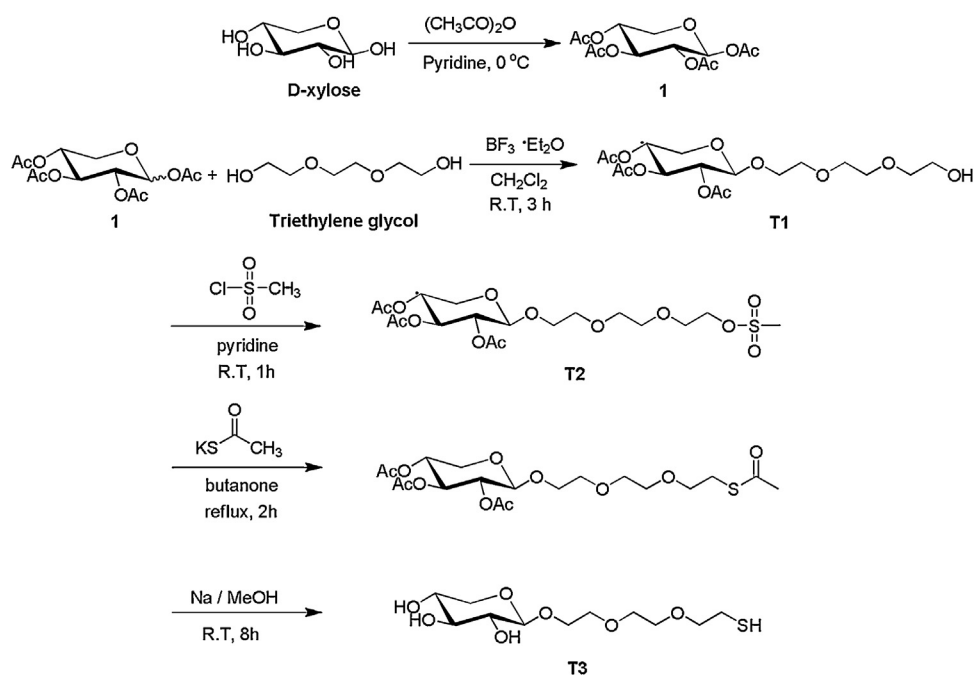
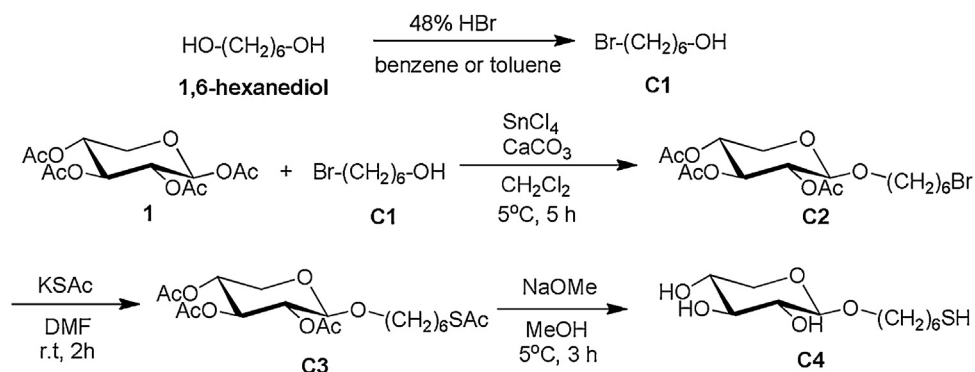


Fig. 1. Thiol derivatives modified on the surface of gold nanoparticles.



Scheme 1. T3 compound synthesis process.



Scheme 2. C4 compound synthesis process.

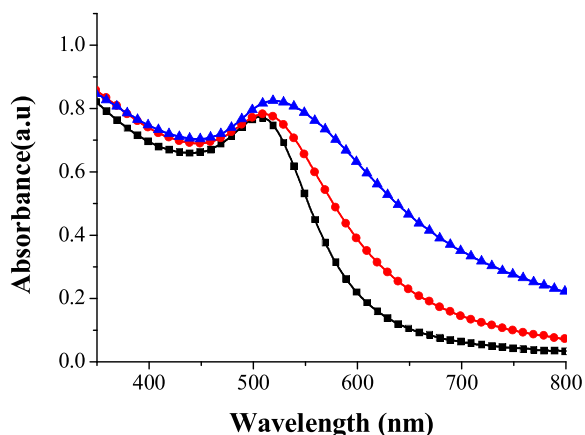


Fig. 2. Ultraviolet visible light absorption diagram of gold nanoparticles modified with thiorides molecules AuNPs-Cit, ● Surface modification of gold nanoparticles on xylose-TEG-SH, ▲ Surface modification of gold nanoparticles on xylose-C₆-SH.

producing non-uniform particle sizes in stable colloidal systems with the help of stabilizers [20]. To date, some compounds have been used to modify AuNPs to improve their stability, dispersibility, and biocompatibility such as surfactants, cyclodextrin, and thiol compounds [21–25]. Among the above compounds, thiol compounds can efficiently enhance the stability and dispersivity of

colloidal AuNPs in aqueous solution. Gao et al. [26] indicated that the thiol groups of these compounds can bind covalently to the surface of AuNPs via a Au – S bond, which consist of glutathione, mercaptopropionic acid, cysteine, cystamine, dihydrolipoic acid, thiol-ending polyethylene glycol, some derivatives, etc. [27–37] Many hydroxyl and carbonyl groups are involved in carbohydrates, they provide a unique H-bonding capabilities of sugar coated nanoparticle in formulating attractive nano construction abilities of supramolecular architecture for establishing smart nanomaterials. Thiol tailored sugars is used as synthons for carbohydrate functionalization of gold nanoparticles in present strategies [38,39]. Roberts et al. [40] utilized reducing agent of sodium borohydride for the synthesis and stabilization of β-D-glucose capped AuNPs. Katti et al. [41] presented the production of AuNPs via traditional sugar coated synthetic strategies which cannot generate aspired results. They exhibited surface coating AuNPs of sugars such as glucose (30 ± 8 nm), sucrose (10 ± 6 nm), maltose (8 ± 2 nm), lactose (3 ± 1 nm), raffinose (6 ± 2 nm), and starch (39 ± 9 nm) with a reducing agent of non-toxic water-soluble phosphino aminoacid. Ribeiro et al. [42] utilized branched polyethyleneimine via primary amine groups substituted by sugar moieties to exhibit an apparent one-spot synthesis of polymer-stabilized ~20 nm AuNPs. Compared the stabilization of unmodified polymer chains, the use of sugar substituted polymer chains produce gold nanocolloids with decreased cytotoxicity and promoted cellular uptake.

Studies for the immobilization of glucose oxidase onto gold nanoparticles surfaces have recently been demonstrated with enhanced activity [43] and binding affinity [44]. Not much effort

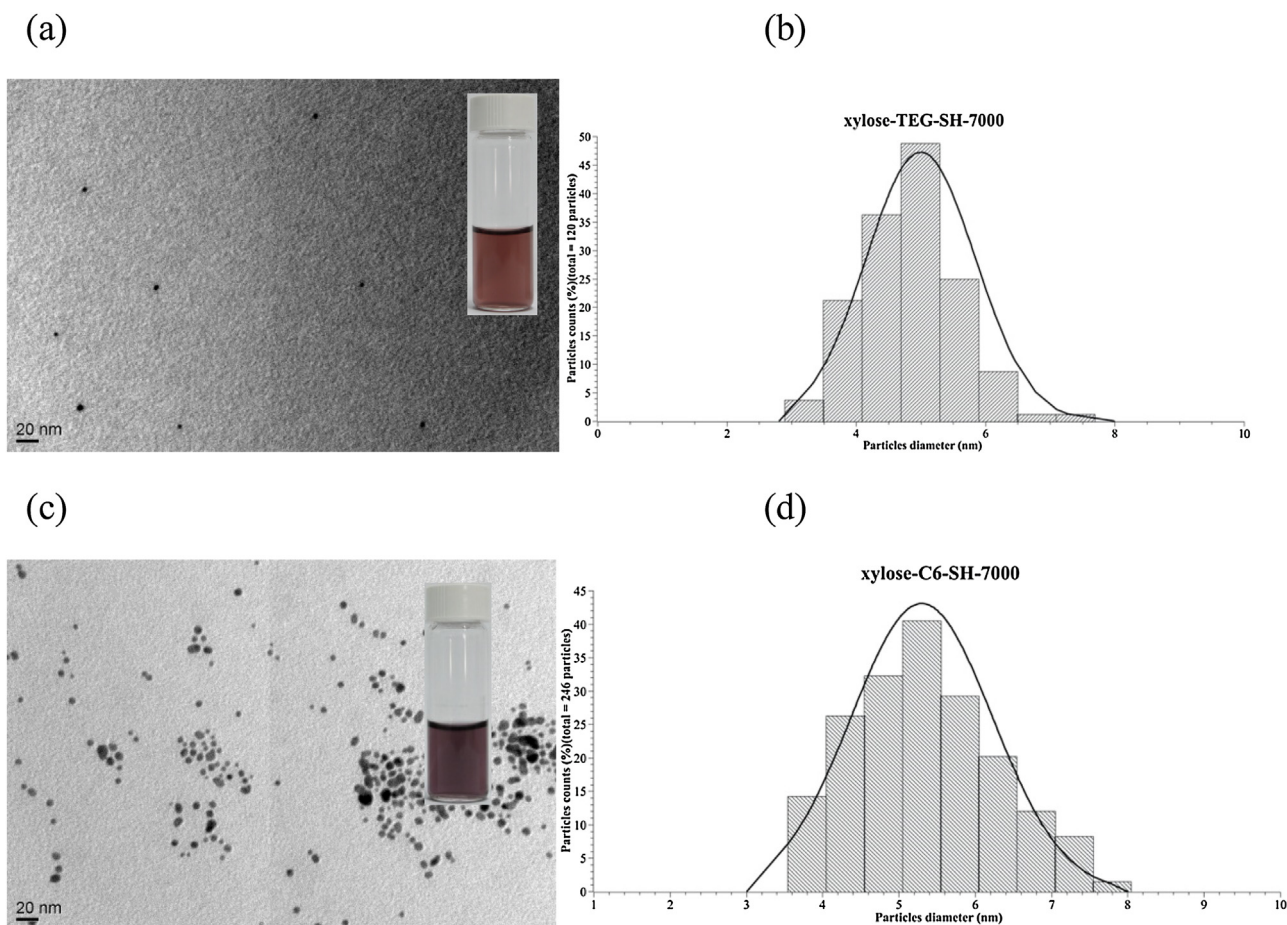


Fig. 3. Surface modification of gold nanoparticles on xylose-TEG-SH (a) TEM and (b) Particle size distribution; Surface modification of gold nanoparticles on xylose-C₆-SH (c) TEM and (d) Particle size distribution.

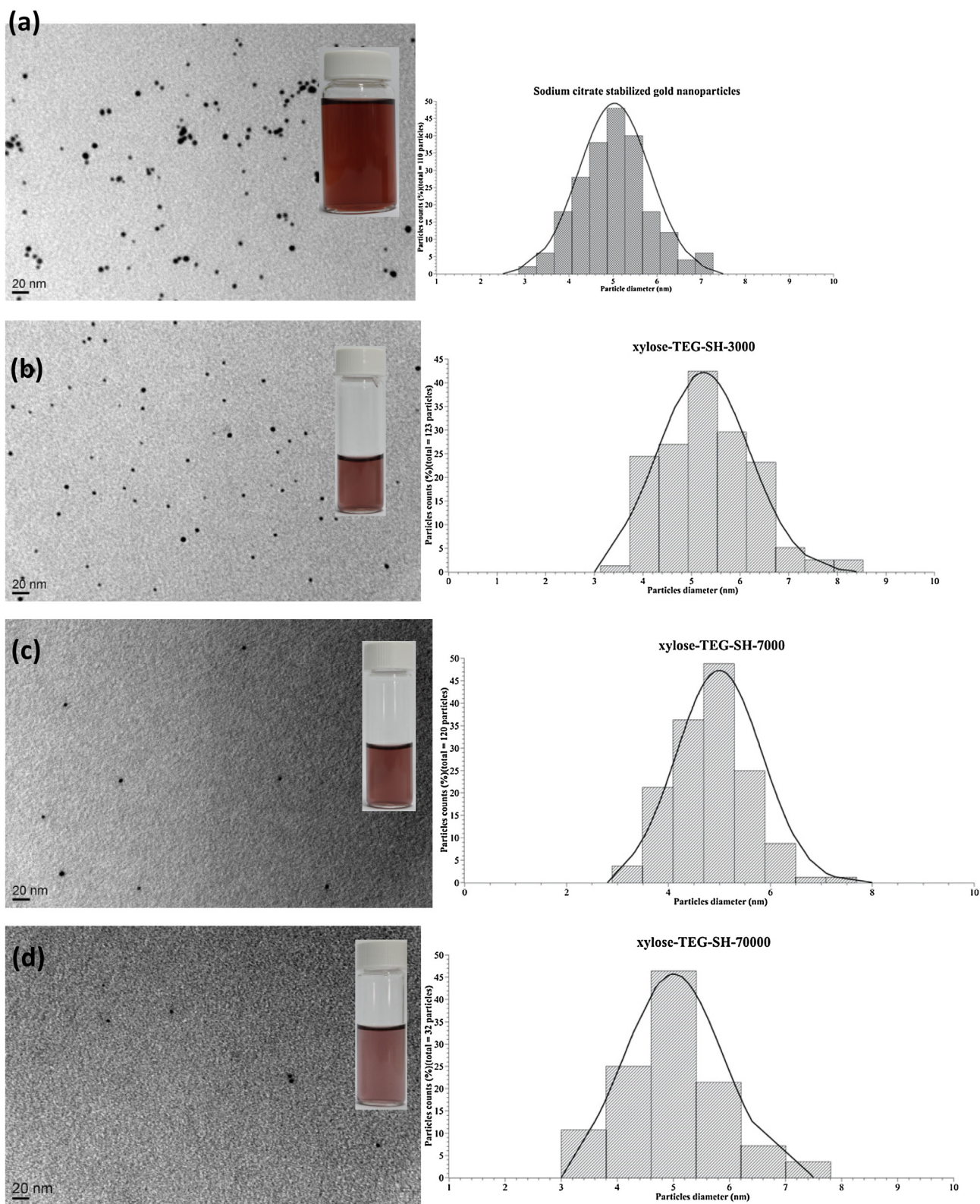


Fig. 4. TEM and particle size distribution of different Xylose-TEG-SH ratio modified to the surface of gold nanoparticles: (a) AuNPs-Cit, $d = 5.0 \pm 0.8$ nm; (b) 1:3000, $d = 5.2 \pm 0.9$ nm; (c) 1:7000, $d = 5.0 \pm 0.8$ nm; (d) 1:70000, $d = 5.0 \pm 0.9$ nm.

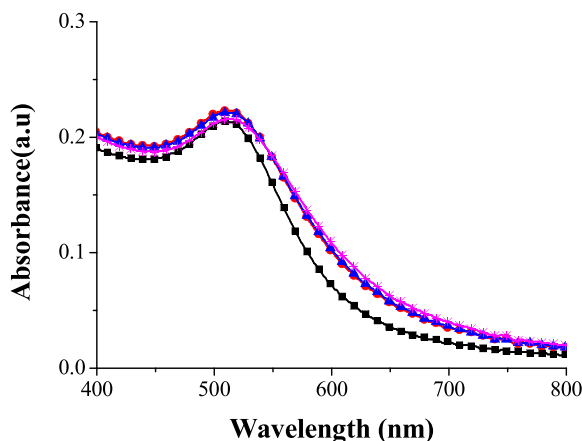


Fig. 5. Ultraviolet visible spectrographs of different Xylose-TEG-SH ratio modified to the surface of gold nanoparticles ■ AuNPs- Na_3Cit , ● AuNPs-SH-TEG-xylose (1:3000).

▲ AuNPs-SH-TEG-xylose (1:7000) ✱ AuNPs-SH-TEG-xylose (1:70000)

has been made to covalently immobilize GOx on biocompatible gold nanoparticles. In this study, we used the seeding growth technique to synthesize AuNPs. The surface of these materials was then decorated with thiolated xylose derivatives. The size of the particles were examined using Correlation Spectroscopy (COSY) and UV-vis spectroscopy. These characteristics are correlated with particle size analysis obtained from transmission electron microscopy (TEM). We investigated the use of untreated AuNPs, and AuNPs conjugated with the surface decorated with thiolated xylose derivatives as to cytotoxic along with their mechanism of action.

2. Materials and methods

2.1. Synthesis of sodium citrate stabilized gold nanoparticles

Sodium citrate stabilized gold nanoparticles (AuNPs-Cit) were prepared using the seeding growth approach [18]. To prevent the accumulation of gold nanoparticles, the coating agent must be added to the reaction system (detailed experimental procedure is discussed in Supplementary Information), in this case the cladding used is tri-sodium citrate. 49.8 mL 2.5×10^{-4} M water solution of tetrachloroquinic acid and 0.2 mL 2.5×10^{-4} M of sodium citrate aqueous solution (the concentration of nano-gold core aqueous solution is 0.01 wt %) were mixed and stirred evenly at room temperature. Then 0.6 mL 0.1 M sodium borate solution was added quickly while stirring, the solution changing from pale yellow to a

red color. After stirring for approximately 2 h, the solution is also red to avoid light degradation at room temperature.

Firstly, an aqueous solution of tetrachloroquinic acid is prepared and NaBH_4 and sodium citrate are used as a reducing agent and coating agent, respectively. As the preparation of gold nanoparticles proceeds, the color of the reaction mixture will be transformed from the original golden-yellow tetrachloroquinic acid solution into a wine-red nanogold aqueous solution.

Nanogold aqueous solution added two thiol derivatives using displacement reaction to replace sodium citrate of the gold nanoparticle surface, acted as the cladding of the gold nanoparticles surface as shown in Fig. 1.

In the synthesis of thiol derivatives of the glycol chain, 1,2,3,4-tetra-*o*-acetyl-D-xylopyranose is firstly synthesized. The product 1 can be obtained by using D-xylose and Acetic anhydride for the amide reaction [45]. The product 1, triethylene glycol and boron trifluoride diethyl etherate react to synthesize the product T1. Then the product T1 reacted with Methanesulfonyl chloride to obtain the first intermediate, followed by reaction with the Potassium thioacetate to obtain the next intermediate, and finally the product T3 can be obtained by sodium and methanol de-acetylation as shown in Scheme 1 [38].

Alternatively, a long carbon chain thiol derivative was synthesized and a bromine reaction of 1,6-hexanediol and HBr was synthesized into 6-bromo-1-hexaneol (product C1). Product C1 and 6-bromo-1-hexaneol, with the addition of tin chloride, were used to synthesize the product C2 at a temperature of 0–5°C condition. Product C2 and potassium thioacetate were then reacted to obtain product C3. Finally, C3 is reacted with NaOMe to eliminate deacetyl synthesized 8-Mercaptohexyl D-xylopyranoside (product C4) as shown in Scheme 2 [46].

2.2. Cytotoxicity test

In vitro cytotoxicity was performed on NIH 3T3 (mouse embryonic cells) cell lines using the 3-(4,5-dimethylthiazol-2-yl)-2,5-diphenyltetrazolium bromide (MTT) assay. NIH 3T3 cells were grown in Dulbecco's modified Eagle's medium (DMEM) containing 10 % fetal bovine serum (FBS). The cells were then seeded into 96-well plates in 200 μL DMEM containing 10 % FBS at plating density of 5000 cells/well and incubated at 37 °C, 5% CO_2 for 24 h prior to addition of test materials. The test materials were added in fresh medium. The fresh medium containing the test materials at concentrations for 1 μM or 100 μM was added into the cells and incubated at 37°C, 5% CO_2 for an additional 24 h. After treatment, 200 μL of MTT (1 mg/ mL) in FBS-free DMEM culture media were added to each well and incubated at 37 °C for 4 h. After removing the medium containing the MTT, the formed formazan crystals were solubilized in 150 μL of dimethyl sulfoxide, and the absorbance at 570 nm was measured using a microplate reader.

Table 1
Gold nanoparticles and gold nanoparticle modified carbohydrate derivatives.

	Plasmon band max (λ ; nm)	measd particle diam (nm)
AuNPs-Cit	506	5.0 \pm 0.8
AuNP-SH-TEG-xylose		
1:3000	510	5.2 \pm 0.9
1:7000	510	5.0 \pm 0.8
1:70000	511	5.0 \pm 0.9
AuNP-SH-C ₆ -xylose		
1:3000	512	5.3 \pm 0.9
1:5000	512.5	5.0 \pm 0.8
1:7000	519.5	5.3 \pm 0.9

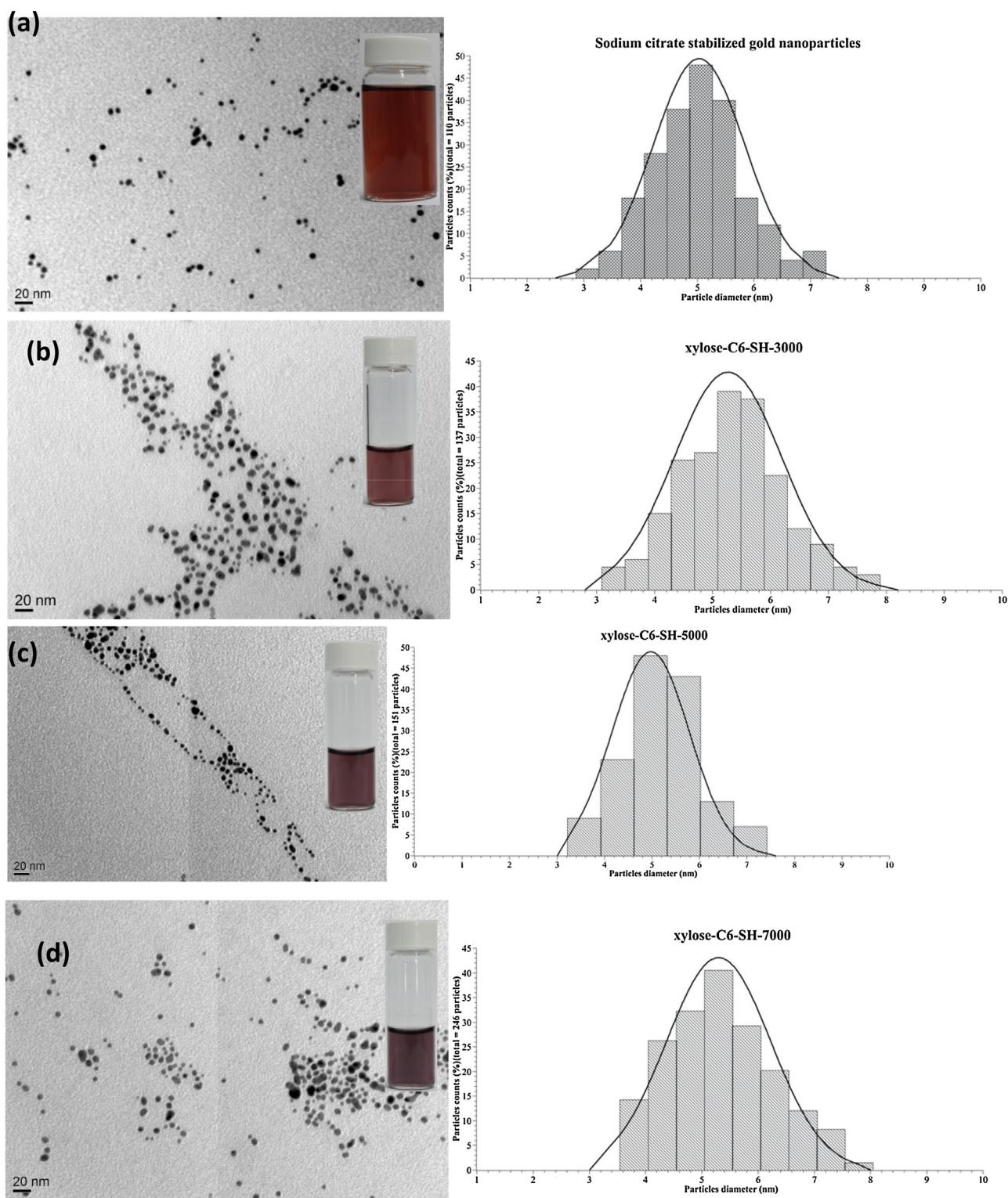


Fig. 6. TEM and particle size distribution of different Xylose-C₆-SH ratio modified to the surface of gold nanoparticles: (a) AuNPs-Cit, 5.0 ± 0.8 nm, (b) 1:3000, d = 5.3 ± 0.9 nm, (c) 1:5000, d = 5.0 ± 0.8 nm, (d) 1:7000, d = 5.3 ± 0.9 nm.

The percentage of cell survival was determined using the following formula:

$$\% \text{ Cell Survival} = \frac{\text{Abs}(\text{test materials})}{\text{Abs}(\text{control})} \times 100$$

where Abs means absorbance at 570 nm.

Experiments were carried out in triplicate and cells containing no test materials served as the control.

3. Results and discussion

3.1. UV-vis analysis and TEM images of thiol derivatives modified in gold nanoparticles

Prepared surface-modified seamount molecules gold nanoparticles for ultraviolet light-visible spectrometer (UV-vis)

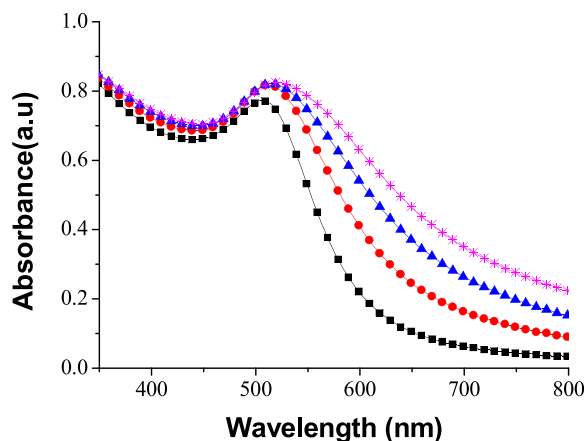


Fig. 7. Ultraviolet visible spectrograph of different Xylose-C₆-SH ratio modified to the surface of gold nanoparticles.

■ AuNPs-Na₃Cit, ● AuNPs-SH-TEG-xylose (1:3000)
▲ AuNPs-SH-TEG-xylose (1:5000), * AuNPs-SH-TEG-xylose (1:7000)

detection, confirmed the surface plasma resonance absorption peak, observed the resonance absorption peak changes between the unmodified gold nanoparticles, confirmed whether the saccharides have been modified on the surface of the gold

nanoparticles, and explored the effects of adding different ratio of the saccharides on the particles. Finally, the cytotoxicity test was performed.

Fig. 2 shows the results of UV-vis analysis, AuNPs-Cit (6.47×10^{-8} M) has a maximum resonance absorption peak (λ_{max}) at 506 nm. An absorption peak caused by limited surface plasma resonance and resulting from the red color of the solution. When xylose-C₆-SH is added to nanogold solution, its color gradually changes from red to purple. From the ultraviolet-visible spectrum, it is known that the red shift of its absorption front position is moved to 519.5 nm, and the absorption peak is wider, approving the creation of gold nanoparticles, and the developing of the peak could be associated to an indirect indication of the presence of thiol on the surface of the gold nanoparticles. The reason for the feature peak red shift is that xylose-C₆-SH is modified on the surface of the gold nanoparticles, and the hydrogen bonds of the thiorium on the surface of the gold nanoparticles cause the attraction between particles, resulting in an aggregated phenomenon [47]. In addition, the absorption peak also widens because xylose-C₆-SH is modified on the surface of the gold nanoparticles to make the particles slightly larger [48]. When xylose-TEG-SH is added to nano-gold solution, the color does not change, the red shift of the resonance absorption peak moves to 510 nm, but the change of red shift and peak widening is not as different as the long carbon chain. The microstructural investigation of the xylose-TEG-SH and

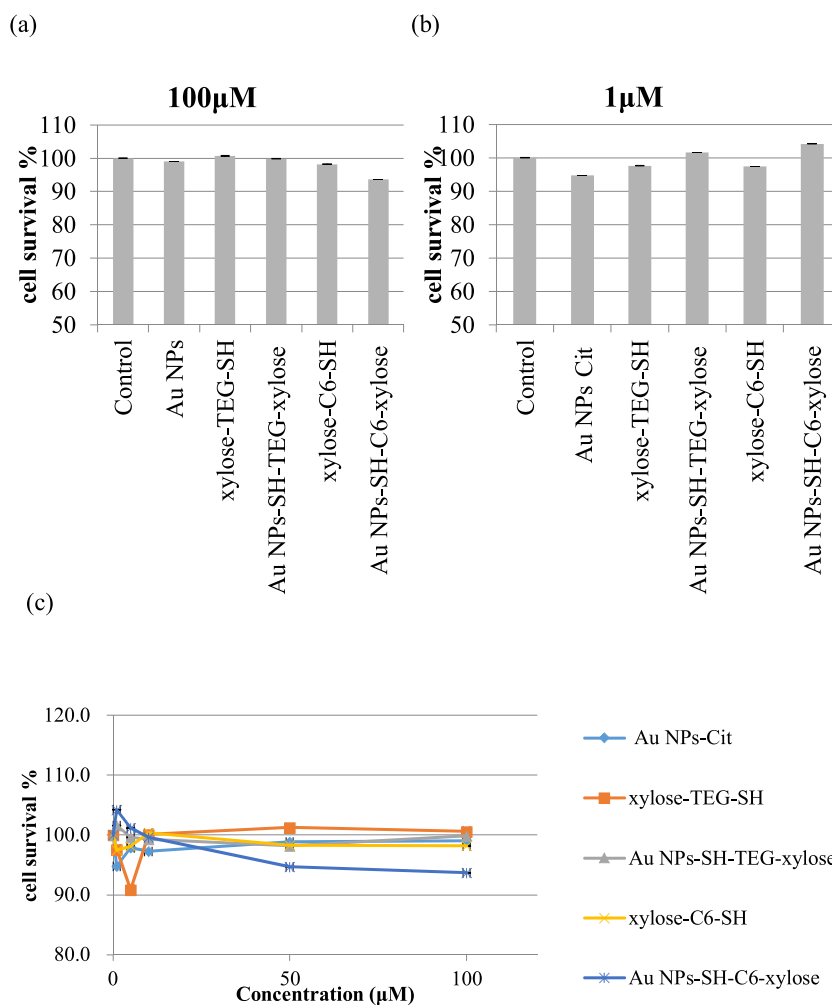


Fig. 8. Cytotoxicity tests: NIH 3T3 cells were subjected to a MTT assay to test the toxicity of the materials, as described in the Materials and Methods. Control, no tested material supplement. (a) survival rate of cells with treatment at concentration for 100 μ M, (b) survival rate of cells with treatment at concentration for 1 μ M, and (c) survival rate of cells with treatment at concentration for 1, 50 and 100 μ M.

xylose-C₆-SH attached gold nanoparticles was performed using the transmission electron microscopy (TEM) images to express the size, shape, and distribution/separation of the particles as shown in Fig. 3. Fig. 3a presents a bright-field electron micrograph of the thiolated gold nanoparticles recorded at a magnification of 3000×, and it is expressed that the nearly spherical xylose-TEG-SH gold nanoparticles are distributed uniformly with a low tendency of agglomeration among the particles [49]. The size of the spherical thiolated gold particles is found to vary from 3 to 7 nm with an average size of about 5 nm as shown in Fig. 3b. The TEM micrograph of the thiolated gold nanoparticles recorded at 3000× magnification attached with a xylose-C₆-SH is shown in Fig. 3c. From the micrographs, it is examined that the size of the particles has increased, with a slightly higher tendency of agglomeration [49], which may be due to the presence of the xylose-C₆-SH. The size of the particles varies from 3 to 7 nm with an average size of 5 nm. The gold nanoparticles modified with xylose-TEG-SH which have a great distance between them and cannot produce aggregation, because the tetra glycol is hydrophilic and highly dispersed in water, and it cannot cause such a significant difference in color and UV-vis as the gold nanoparticles that are modified with xylose-C₆-SH.

To change the ratio of carbohydrate molecules available for the modification of the gold nanoparticles in solution, the ratio of xylose-TEG-SH addition was changed in the following sequence: 1:3000, 1:7000, 1:70000 (AuNPs: xylose-TEG-SH), the TEM and particle size distribution are shown in Fig. 4. When the ratio was changed, there was no difference in either dispersion or particle size. Fig. 5 shows the results of UV-vis analysis, a modified nano-gold solution causes a red shift of 4–5 nm surface plasma resonance absorption peaks, and when the added ratio increases (1:3000–1:70000), the resonance absorption peak is only slightly wider and more displaced. Kadir and Víctor [41] modified gold particles using polyoxyethylene (20) sorbitan monolaurate, causing only a red shift of 3 nm. Using 16-mercaptodecanoic acid for the Modification of gold nanoparticles resulted in a red shift of 30 nm. Continuing two common modifications to the surface of the gold particles will cause a red shift of 4–5 nm, which the difference of red shift phenomena is generated by the dielectric constant of the environment of the gold nanoparticles and the phenomenon of the reunion between particles.

Then changed the adding xylose-C₆-SH ratio in the order: 1:3000, 1:5000, 1:7000 (AuNPs: xylose-C₆-SH). The results of TEM and particle size distribution are shown in Fig. 6. It is observed that there is a aggregated phenomenon between the modified gold nanoparticles in solution and the intensity of the color of the solution increases toward to purple, the particle size distribution did not discernably changed. Fig. 7 and Table 1 presents the results of UV-vis analysis, showing that a modified gold nanoparticle solution causes the red shift of the surface plasma resonance absorption peak and widen. While the added ratio increased (1:3000–1:7000), the peak would be more red and the peak would be wider due to the effect of the aggregated phenomenon between the gold nanoparticles and the influence of the surrounding dielectric constant [47].

3.2. Cytotoxicity test

The cytotoxicity test was performed to check the biocompatibility of nano-gold solution, two carbohydrate derivatives and modified nano-gold solution (Fig. 8). The MTT assay on NIH 3T3 cell lines confirmed that all the test materials showed no toxicity with the more than 90 % of cell viability in both low concentration (1 μM) and high concentration (100 μM), compared with the control.

4. Conclusion

We successfully synthesized two thiol derivatives, the compounds T3 and C4, using the end of the thiol base (-SH) to modify the derivatives on the surface of gold nanoparticles. When the saccharides are successfully modified on the surface of the gold nanoparticles, they changed the surface plasma resonance and ambient dielectric constant of the particles, resulting in absorption peak displacement and wave width changes.

When the gold nanoparticles are modified with hydrophobic long carbon chain of the carbohydrate molecules, the phenomenon of particle aggregation occurs, resulting in the resonance absorption peak red shift and an increase in the width of the peak. When the surface of the gold particles are modified with hydrophilic glycol chains of the carbohydrate molecules, the particles will be quite dispersed when in an aqueous solution. Under these conditions there will be no aggregation between the particles, so the change in resonance absorption peak position and wave width is negligible. As the proportion of carbohydrate derivatives is increased, the phenomenon of particle aggregation is further reduced to a point where the resonance absorption peak and wave width are unchanged.

The nano-gold solution, two carbohydrate derivatives and modified nano-gold solution were tested for cytotoxicity to check the biocompatibility. The MTT assay on NIH 3T3 cell lines confirmed that all the test materials showed no toxicity with the more than 90 % of cell viability in both low concentration (1 μM) and high concentration (100 μM), compared with the control.

Declaration of Competing Interest

The authors report no declarations of interest.

Acknowledgements

The authors would like to acknowledge the supports from National Taipei University of Technology with contract number NTUT-TMU-98-11.

Appendix A. Supplementary data

Supplementary material related to this article can be found, in the online version, at doi:<https://doi.org/10.1016/j.btre.2020.e00549>.

References

- [1] M. Delbianco, P. Bharate, S. Varela-Aramburu, P.H. Seeberger, Carbohydrates in supramolecular chemistry, *Chem. Rev.* 116 (2016) 1693–1752.
- [2] M. Marradi, F. Chiodo, I. García, S. Penadés, Glyconanoparticles as multifunctional and multimodal carbohydrate systems, *Chem. Soc. Rev.* 42 (2013) 4728–4745.
- [3] K. Saha, S.S. Agasti, C. Kim, X. Li, V.M. Rotello, Gold nanoparticles in chemical and biological sensing, *Chem. Rev.* 112 (2012) 2739–2779.
- [4] S. Mandal, Synthesis of radioactive gold nanoparticle in surfactant medium, *J. Radioanal. Nucl. Chem.* 299 (2014) 1209–1212.
- [5] F. Porta, M. Rossi, Gold nanostructured materials for the selective liquid phase catalytic oxidation, *J. Mol. Catal. A Chem.* 204 (2003) 553–559.
- [6] Y.Y. Yu, S.S. Chang, C.L. Lee, C.R. Wang, Gold nanorods: electrochemical synthesis and optical properties, *J. Phys. Chem. B* 101 (1997) 6661–6664.
- [7] M. Nakanishi, H. Takatani, Y. Kobayashi, F. Hori, R. Taniguchi, A. Iwase, R. Oshima, Characterization of binary gold/platinum nanoparticles prepared by sonochemistry technique, *Appl. Surf. Sci.* 241 (2005) 209–212.
- [8] S. Eustis, M.A. El-Sayed, Why gold nanoparticles are more precious than pretty gold: noble metal surface plasmon resonance and its enhancement of the radiative and nonradiative properties of nanocrystals of different shapes, *Chem. Soc. Rev.* 35 (2006) 209–217.
- [9] A.J. Haes, W.P. Hall, L. Chang, W.L. Klein, R.P. Van Duyne, A localized surface plasmon resonance biosensor: first steps toward an assay for Alzheimer's disease, *Nano Lett.* 4 (2004) 1029–1034.

- [10] M.P. Pileni, Nanosized particles made in colloidal assemblies, *Langmuir* 13 (1997) 3266–3276.
- [11] K. Okitsu, M. Ashokkumar, F. Grieser, Sonochemical synthesis of gold nanoparticles: effects of ultrasound frequency, *J. Phys. Chem. B* 109 (2005) 20673–20675.
- [12] S.R. Hall, W. Shenton, H. Engelhardt, S. Mann, Site-specific organization of gold nanoparticles by biomolecular templating, *Chem Phys Chem* 2 (2001) 141–191.
- [13] M.H. Magnusson, K. Deppert, J.O. Malm, J.O. Bovin, L. Samuelson, Gold nanoparticles: production, reshaping, and thermal charging, *J Nano Res.* 1 (1999) 243–251.
- [14] J. Turkevich, G. Garton, P.C.J. Stevenson, The color of colloidal gold, *Colloid Sci.* 9 (1954) 26.
- [15] G. Frens, Controlled nucleation for the regulation of the particle size in monodisperse gold suspensions, *Nature* 241 (1973) 20–22.
- [16] M. Brust, M. Walker, D. Bethell, D.J. Schiffrin, R. Whyman, Synthesis of thiol-derivatised gold nanoparticles in a two-phase liquid–liquid system, *Chem. Commun.* 7 (7) (1994) 801–802.
- [17] K.R. Brown, D. G. Walter, M. J. Natan, Seeding of colloidal Au nanoparticle solutions. 2. Improved control of particle size & shape, *Chem. Mater.* 12 (2) (2000) 306–313.
- [18] N.R. Jana, L. Gearheart, C. J. Murphy, Seeding growth for size control of 5–40 nm diameter gold nanoparticles, *Langmuir* 17 (22) (2001) 6782–6786.
- [19] K.H. Tan, H.A. Tajuddin, M.R. Johan, Feasibility study on the use of the seeding growth technique in producing a highly stable gold nanoparticle colloidal system, *J. Nanomater.* (2015) 537125 Article ID.
- [20] N.R. Jana, L. Gearheart, C.J. Murphy, Evidence for seed mediated nucleation in the chemical reduction of gold salts to gold nanoparticles, *Chem. Mater.* 13 (7) (2001) 2313–2322.
- [21] Y.Y. Zhao, Z. Wang, W. Zhang, X.Y. Jiang, Adsorbed tween 80 is unique in its ability to improve the stability of gold nanoparticles in solutions of biomolecules, *Nanoscale* 2 (2010) 2114–2119.
- [22] D. Sharma, A biologically friendly single step method for gold nanoparticle formation, *Colloids Surf., B* 85 (2011) 330–337.
- [23] M. Tarantola, A. Pietuch, D. Scheneider, J. Rother, E. Sunnick, C. Rosman, S. Pierrat, C. Sonnichsen, J. Wegener, A. Janshoer, Toxicity of gold-nanoparticles: synergistic effects of shape and surface functionalization on micromotility of epithelial cells, *Nanotoxicology* 5 (2) (2011) 254–268.
- [24] M. Ortiz, A. Fragoso, C.K. O'Sullivan, Detection of Antigliadin Autoantibodies in celiac patient samples using a cyclodextrin-based supramolecular biosensor, *Anal. Chem.* 83 (8) (2011) 2931–2938.
- [25] D. Joseph, K.E. Geckeler, Surfactant-directed multiple anisotropic gold nanostructures: synthesis and surface-enhanced raman scattering, *Langmuir* 25 (22) (2009) 13224–13231.
- [26] D.H. Tsai, F.W. DelRio, R.I. MacCuspie, T.J. Cho, M.R. Zachariah, V.A. Hachley, Competitive adsorption of thiolated polyethylene glycol and mercaptopropionic acid on gold nanoparticles measured by physical characterization methods, *Langmuir* 26 (12) (2010) 10325–10333.
- [27] H. Lee, S.H. Choi, T.G. Park, Direct visualization of hyaluronic acid polymer chain by self-assembled one-dimensional array of gold nanoparticles, *Macromolecules* 39 (1) (2006) 23–25.
- [28] C.M. Ruan, W. Wang, B.H. Gu, Surface-enhanced Raman scattering for perchlorate detection using cystamine-modified gold nanoparticles, *Anal. Chim. Acta* 567 (1) (2006) 114–120.
- [29] S.X. Zhang, N. Wang, H.J. Yu, Y.M. Niu, C.Q. Sun, Covalent attachment of glucose oxidase to an Au electrode modified with gold nanoparticles for use as glucose biosensor, *Bioelectrochemistry* 67 (2005) 15–22.
- [30] S. Roux, B. Garcia, J.L. Bridot, M. Salomé, C. Marquette, L. Lemelle, P. Gillet, L. Blum, P. Perriat, O. Tillement, Synthesis, characterization of dihydrolipoic acid capped gold nanoparticles, and functionalization by the electroluminescent luminol, *Langmuir* 21 (6) (2005) 2526–2536.
- [31] B.C. Mei, K. Susumu, I.L. Medintz, J.B. Delehanty, T.J. Mountziaris, H. Mattoussi, Modular poly(ethylene glycol) ligands for biocompatible semiconductor and gold nanocrystals with extended pH and ionic stability, *J. Mater. Chem.* 18 (2008) 4949–4958.
- [32] F. Chai, C.G. Wang, T.T. Wang, L. Li, Z.M. Su, Colorimetric detection of Pb²⁺ using glutathione functionalized gold nanoparticles, *ACS Appl. Mater. Interfaces* 2 (5) (2010) 1466–1470.
- [33] P. Ghosh, G. Han, M. De, C.K. Kim, V.M. Rotello, Gold nanoparticles in delivery applications, *Adv. Drug Delivery Rev.* 60 (11) (2008) 1307–1315.
- [34] E.D. Kaufman, J. Belyea, M.C. Johnson, Z.M. Nicholson, J.L. Richs, P.K. Shah, M. Bayless, T. Pettersson, Z. Feldotó, E. Blomberg, P. Claesson, S. Franzen, Probing protein adsorption onto mercaptoundecanoic acid stabilized gold nanoparticles and surfaces by quartz crystal microbalance and ζ-Potential measurements, *Langmuir* 23 (11) (2007) 6053–6062.
- [35] F.Q. Hu, Y.L. Ran, Z.A. Zhou, M.Y. Gao, Preparation of bioconjugates of CdTe nanocrystals for cancer marker detection, *Nanotechnology* 17 (12) (2006) 2972–2977.
- [36] H.W. Huang, X.Y. Liu, T. Hu, P.K. Chu, Ultra-sensitive detection of cysteine by gold nanorod assembly, *Biosens. Bioelectron.* 25 (9) (2010) 2078–2083.
- [37] M.H. Stewart, K. Susumu, B.C. Mei, I.L. Medintz, J.B. Delehanty, J.B. Blanco-Canosa, P.E. Dawson, H. Mattoussi, Multidentate poly(ethylene glycol) ligands provide colloidal stability to semiconductor and metallic nanocrystals in extreme conditions, *J. Am. Chem. Soc.* 132 (28) (2010) 9804–9813.
- [38] A.J. Reynolds, A.H. Haines, D.A. Russell, Gold glyconanoparticles for mimics and measurement of metal ion-mediated carbohydrate–carbohydrate interactions, *Langmuir* 22 (3) (2006) 1156–1163.
- [39] J.M. De la Fuente, P. Eaton, A.G. Barrientos, M. Menendez, S. Penades, *J. Am. Chem. Soc.* 127 (2005) 6192–6197.
- [40] J.C. Liu, M. Anand, C.B. Roberts, Synthesis and extraction of β-d-glucose-stabilized Au nanoparticles processed into low-defect, wide-area thin films and ordered arrays using CO₂-Expanded liquids, *Langmuir* 22 (2006) 3964–3971.
- [41] K.K. Katti, V. Kattumuri, S. Bhaskaran, K.V. Katti, R. Kannan, Facile and general method for synthesis of sugar coated gold nanoparticles, *Int. J. Green Nanotechnol. Biomed.* 1 (1) (2009) B53–B59.
- [42] C.A.S. Ribeiro, L.J.C. Albuquerque, C.E. de Castro, B.L. Batista, A.L.M. de Souza, B.L. Albuquerque, M.S. Zilsec, I.C. Bellettin, C. Fernando, F.C. Giacomelli, *Colloids Surf. A* 580 (2019) 123690.
- [43] P. Pandey, S.P. Singh, S.K. Arya, V. Gupta, M. Datta, S. Singh, B.D. Malhotra, *Langmuir* 23 (2007) 3333–3337.
- [44] Masauso Moses Phiri, Danielle Wingrove Mulder, Shayne Mason, Barend christiaan vorster, *R. Soc. Open Sci.* 6 (5) (2019) 190205.
- [45] M. Gao, Y. Chen, S. Tan, J.H. Reibenspies, R.A. Zingaro, Syntheses of 1-thio-D-xylose and D-ribose esters of diorganoarsinous acids and their anticancer activity, *Heteroa. Chem.* 19 (2) (2008) 199–206.
- [46] T. Murakami, R. Hirono, Y. Sato, K. Furusawa, Efficient synthesis of ω-mercaptoalkyl 1,2-trans-glycosides from sugar peracetates, *Carbohydr. Res.* 342 (8) (2007) 1009–1020.
- [47] Y. Sato, T. Murakami, K. Yoshioka, O. Niwa, 12-Mercaptododecyl β-maltoside-modified gold nanoparticles: specific ligands for concanavalin A having long flexible hydrocarbon chains, *Analyt. Bioanal. Chem.* 391 (2008) 2527–2532.
- [48] A. Kadir, H. Víctor Pérez-Luna, Surface modification of colloidal gold by chemisorption of alkanethiols in the presence of a nonionic surfactant, *Langmuir* 18 (16) (2002) 6059–6065.
- [49] P. Pandey, S.P. Singh, S.K. Arya, V. Gupta, M. Datta, S. Singh, B.D. Malhotra, Application of thiolated gold nanoparticles for the enhancement of glucose oxidase activity, *Langmuir* 23 (6) (2007) 3333–3337.